TIME DOMAIN SYNCHRONIZATION AND DECODING OF P1 SYMBOL IN DVB-T2

Mingchao Yu, Parastoo Sadeghi

Research School of Information Sciences and Engineering, The Australian National University
Canberra, ACT, Australia 0200
Email: {ming.yu}, {parastoo.sadeghi}@anu.edu.au

ABSTRACT

In this paper we propose a novel timing and frequency synchronization and decoding method for the P1 symbol in DVB-T2 based on the correlation between the received signal and the time domain P1 symbols. This method does not require post-FFT decoding and is insensitive to the frequency-shift offset and continuous-wave (CW) interference. The performance of the proposed method is evaluated via computer simulations, which shows that not only does it achieve good synchronization performance, but also it provides a decoding SNR gain of at least 6dB in AWGN channel and at least 2dB in multipath Rayleigh fading channel compared with the performance reported in the standard guidelines.

Index Terms— OFDM, DVB-T2, synchronization, decoding

1. INTRODUCTION

In most orthogonal-frequency-division-multiplexing (OFDM) systems, the time domain (TD) OFDM symbol is the superposition of modulated data and pilot symbols. Employing this property, the correlation between the received signal and the TD symbol of frequency domain pilots (FPTC) was first used in [1] for channel impulse response (CIR) estimation and then in [2] for timing synchronization. A full synchronization scheme was later proposed in [3]. These methods are recommended for the synchronization of normal OFDM symbols in the implementation guideline [4] of the second generation digital terrestrial television broadcasting system (DVB-T2) [5].

In DVB-T2, a preamble OFDM symbol called P1 symbol which carries the basic system information such as transmission mode and FFT size is transmitted before each frame of normal OFDM symbols. To work under severe transmission conditions, two replicas of the main part are frequency-shifted by f_{sh} to form the head and tail of the TD P1 symbol. [4] demonstrates a baseline detection and synchronization scheme based on the correlation between different parts of the received signal, followed by a post-FFT decoding process. Most P1 processing methods in the literature employ the same correlation method. They mainly focus on timing synchronization without being concerned about decoding.

However, since there are only 128 possible patterns for P1 active sub-carriers in the frequency domain (FD), a TD P1 symbol can be treated as the superposition of an all-zero data symbol and 1 of the 128 modulated pilot symbols. Thus based on the correlation between the received signal and TD P1 pilot symbols, we propose a novel P1 synchronization and decoding method. This method is insensitive to f_{sh} offset and CW interference. Post-FFT decoding is also avoided and computer simulations show that it achieves a decoding SNR gain of at least 6dB in AWGN channel and at least 2dB in multipath Rayleigh fading channel compared with the decoding performance given in the guidelines [4].

The paper is organized as follows: Section 2 introduces system model, including P1 symbol properties and the modeling of the received signal. Section 3 presents the proposed method in the order of processing at the receiver. Simulation results are presented in Section 4. Section 5 concludes the paper.

2. SYSTEM MODEL

2.1. Frequency domain P1 symbol

In the frequency domain, a P1 symbol encodes 7 bits. The first 3 bits, from [0 0 0] to [1 1 1], form a sub-sequence called $S1$, indicating transmission mode. The remaining 4 bits form $S2$, carrying information about FFT size. Hence there are 128 possible combinations of $S1$ and $S2$, corresponding to 128 different binary complementary sequences [5] mss_{seq} with length 384. The autocorrelation of mss_{seq} is a delta function with a factor of 384, while the cross-correlation between different mss_{seq} is always zero. mss_{seq} is then DBPSK modulated and scrambled to form the active sub-carriers of a 1K (K=1024) OFDM symbol $\mathbf{X}_p$. $\mathbf{X}_p$ is OFDM modulated to form the main part $\mathbf{p}$ of a TD P1 symbol as:

$$\mathbf{p}(i) = \frac{1}{\sqrt{384}} \sum_{n=0}^{1023} \mathbf{X}_p(n) e^{j2\pi \frac{ni}{1024}}, \qquad i = [0 \sim 1023] \quad (1)$$

Here $[m \sim n]$ means an index sequence from m to n. A detailed encoding process is demonstrated in [5].

2.2. Time domain P1 symbol

In the time domain, a replica of the first 542 and the last 482 samples of $\mathbf{p}$ is frequency shifted by f_{sh} then padded before and after $\mathbf{p}$, respectively, to form the transmitted P1 symbol $\mathbf{x}$:

$$\mathbf{x}(i) = \begin{cases} \mathbf{p}(i) e^{j2\pi \frac{i f_{sh}}{1024}} & i \in C2 = [0 \sim\ 541] \\ \mathbf{p}(i - 542) & i \in C1 = [542 \sim 1083] \\ \mathbf{p}(i - 542) & i \in B1 = [1084 \sim 1565] \\ \mathbf{p}(i - 1024) e^{j2\pi \frac{i f_{sh}}{1024}} & i \in B2 = [1566 \sim 2047] \end{cases} \quad (2)$$

where $f_{sh} = 1/1024T$ and T is the time domain sample spacing.

Obviously there are 128 possible $\mathbf{x}$ sequences, we label them as $\mathbf{x}_0$, $\mathbf{x}_1$, to $\mathbf{x}_{127}$, corresponding to $[S_1\ S_2] = [0000000]$, $[0000001]$, $\cdots$, $[1111111]$. The correlation properties of $\mathbf{x}$ is shown in Fig. 1. The autocorrelation function has an overwhelming correlation peak

This work was supported under Australian Research Council's Discovery Projects funding scheme (project no. DP0773898)

when $t = 0$ which is similar to a delta function. This property enables us to use TD P1 symbols for P1 synchronization. On the other hand, the magnitude of cross-correlation function is much lower than the autocorrelation function, enabling time domain P1 decoding.

We further define a "coarse" P1 symbol $\mathbf{x}_{128}$ which is the average of all $\mathbf{x}$ sequences and hence is known by the receiver:

$$\mathbf{x}_{128} = \overline{\mathbf{x}}_{0\sim127} = \frac{1}{128}\sum_{k=0}^{127}\mathbf{x}_k \tag{3}$$

Due to the above correlation properties, $\mathbf{x}_{128}$ has a correlation peak with every P1 symbol when the timing is correct and has a small correlation when the timing is incorrect. This property is important because it provides a way to do TD synchronization without knowing which P1 symbol is transmitted.

2.3. The received signal

The imperfect channel output $\mathbf{r}_c$ can be modeled as:

$$\mathbf{r}_c = \mathbf{x} * \mathbf{h} + \mathbf{n} \tag{4}$$

Here * denotes convolution. The CIR $\mathbf{h}$ is a scalar equal to 1 in AWGN channel. In multipath Rayleigh fading channel $\mathbf{h}$ is a vector of T-spaced channel taps with complex Gaussian distributed channel gains. $\mathbf{n}$ consists of i.i.d. complex AWGN noise with variance σ^2.

Then a carrier frequency offset (CFO) due to oscillator mismatch between the transmitter and the receiver is introduced to the received signal as:

$$\mathbf{r}(d) = \mathbf{r}_c(d)\cdot\exp\left(j2\pi\frac{\nu d}{1024} + \phi_0\right) \tag{5}$$

Here ν is the CFO normalized by $1/1024T$ with integer part ν_I and fractional part ν_f. ϕ_0 is an arbitrary carrier phase factor. d is the timing index where $d = 0$ corresponds to the correct start of a TD P1 symbol assuming correct sampling clock frequency. We further define a length 2K working sequence $\mathbf{y}$ starting from $\mathbf{r}(d)$:

$$\mathbf{y}_d = \mathbf{r}(d) \sim \mathbf{r}(d + 2047) \tag{6}$$

3. PROPOSED METHOD

For convenience of analysis, we first assume that:

- a P1 symbol $\mathbf{x}_p$ belonging to $\mathbf{x}_{0\sim127}$ is transmitted and is known by the receiver. Such knowledge on $\mathbf{x}_p$, as we will explain later, can be replaced by $\mathbf{x}_{128}$ in practical use;
- the samples before and after $\mathbf{x}_p$ are from normal OFDM symbols with the same power as P1 symbols. This assumption is also true in real DVB-T2 systems;
- the channel is AWGN, i.e., $\mathbf{h} = 1$. The performance in multipath Rayleigh fading channel will be discussed in Section 4.

Under these assumptions, $\mathbf{y}_d$ becomes:

$$\mathbf{y}_d(i) = \mathbf{x}(d+i)e^{j2\pi\frac{\nu(d+i)}{1024}+\phi_0} + \mathbf{n}(i), \quad i = [0\sim2047] \tag{7}$$

where:

$$\mathbf{x}(i) = \begin{cases}\mathbf{x}_p(i) & i = [0\sim2047]\\ \textit{random value} & \text{otherwise}\end{cases} \tag{8}$$

Now we are ready to introduce the correlation $\mathbf{z}_d$ between the received signal $\mathbf{y}_d$ and TD P1 symbol $\mathbf{x}_p$ as:

$$\begin{aligned}\mathbf{z}_d(i) &= \mathbf{y}_d(i)\cdot\mathbf{x}_p^*(i), \qquad i = [0\sim2047]\\ &= \mathbf{x}(d+i)\mathbf{x}_p^*(i)e^{j2\pi\frac{\nu(d+i)}{1024}+\phi_0} + \mathbf{n}(i)\mathbf{x}_p^*(i)\end{aligned} \tag{9}$$

where $(\cdot)^*$ denotes complex conjugation.

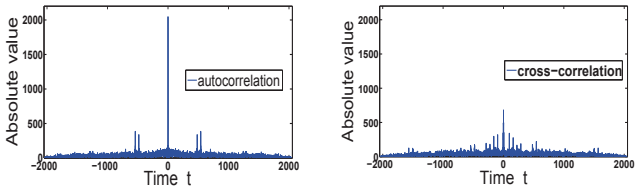

(a) autocorrelation function (b) cross-correlation function

Fig. 1. Time domain correlation property of P1 symbols

3.1. Coarse timing and frequency synchronization

When the timing is correct, i.e., $d = 0$, $\mathbf{z}_d$ can be written as:

$$\mathbf{z}_0(i) = |\mathbf{x}_p(i)|^2 e^{j2\pi\frac{\nu i}{1024}+\phi_0} + \mathbf{n}(i)\mathbf{x}_p^*(i), \quad i = [0\sim2047] \tag{10}$$

After multiplying with noise $\mathbf{n}$, the distinctive frequency components in $\mathbf{x}_p^*$, i.e., the active sub-carriers, in the second term of the righthand side of (10) is distributed across all frequencies in $\mathbf{z}_0$. Hence the only distinctive frequency component in $\mathbf{z}_0$ is ν. On the other hand, when $d \neq 0$ or there is no P1 symbol, $\mathbf{z}_d$ will not have a distinctive frequency component. Hence, the existence of such frequency component in $\mathbf{z}_d$ can be used as a metric for P1 detection and coarse timing synchronization (CTS), while the distinctive frequency value can be used for coarse frequency synchronization (CFS).

To identify such frequency component in a working sequence, [6] proposed a direct trial-and-error frequency search method on OFDM training symbols which is time-consuming depending on the search resolution. However, we find that the frequency search can be efficiently implemented by a 2K FFT on $\mathbf{z}_d$. We denote the magnitude of the length 2K FFT output sequence as $\mathbf{Z}_d$:

$$\mathbf{Z}_d(k) = \left|\sum_{i=0}^{2047}\mathbf{z}_d(i)e^{-j2\pi\frac{ik}{2048}}\right|, \quad k = [0\sim2047] \tag{11}$$

We first show how our frequency search method works if ν is a multiple of 0.5. Suppose $n = 2\nu$. When $d = 0$, by substituting (10), the n^{th} FFT output $\mathbf{Z}_0(n)$ becomes:

$$\begin{aligned}\mathbf{Z}_0(n) &= \left|\sum_{i=0}^{2047}\left[|\mathbf{x}_p(i)|^2 e^{j2\pi\frac{\nu i}{1024}+\phi_0} + \mathbf{n}(i)\mathbf{x}_p^*(i)\right]e^{-j2\pi\frac{ni}{2048}}\right|\\ &= \left|e^{\phi_0}\left[\sum_{i=0}^{2047}|\mathbf{x}_p(i)|^2 e^{j2\pi\frac{\nu i}{1024}-j2\pi\frac{\nu i}{1024}} + \mathbf{n}'(i)\right]\right|\\ &= \sum_{i=0}^{2047}|\mathbf{x}_p(i)|^2\end{aligned} \tag{12}$$

The last equation holds because $\mathbf{n}'(i) = \mathbf{n}(i)\mathbf{x}_p^*(i)e^{-j2\pi\frac{ni}{2048}-\phi_0}$ is still AWGN noise and its sum over thousands of samples is statistically zero. In (12), FFT process compensates for CFO in the n^{th} output $\mathbf{Z}_0(n)$, and its magnitude, $\sum_{i=0}^{2047}|\mathbf{x}_p(i)|^2$, is the maximum value we can get. Such compensation and maximization does not happen in other $\mathbf{Z}_0(k)$ where $k \neq n$, as shown in Fig. 2(a). Moreover, when there is no distinctive frequency component in $\mathbf{z}_0$ due to wrong timing or due to the absence of P1 symbol, such compensation and maximization does not happen, either, as shown in Fig. 2(b).

CFO is unlikely to be an integer in reality, so there will be residual fractional CFO remaining in (12). Since 2K FFT is performed over $2048T$, our normalized frequency search resolution is

0.5, implying that the residual ν_f is no more than ± 0.25 and thus the equality in (12) should be replaced by approximation. In the worst case that ν_f is 0.25 before FFT, there will be two distinctive FFT outputs, $\mathbf{Z}_0(2\nu \pm 0.5)$, with the same magnitude that is larger than $\sum_{i=0}^{2047} |\mathbf{x}_p(i)|^2/2$. They do not degrade the CTS performance because both of them are sufficiently larger than the rest FFT outputs when $d = 0$ and all the FFT outputs when $d \neq 0$. For CFS, $\nu_{i,est} = \nu \pm 0.25$ are both acceptable and the residual ν_f is ∓ 0.25.

Next, the ratio between $\max_k\{\mathbf{Z}_d(k)\}$ and $\sum_{k=0}^{2047} \mathbf{Z}_d(k)$ can be used to indicate whether there is a "distinctive" frequency component or not in a given $\mathbf{Z}_d$. But considering $\sum_{k=0}^{2047} \mathbf{Z}_d(k)$ is statistically invariant, $\max_k\{\mathbf{Z}_d(k)\}$ is a sufficient criterion. Hence, our CTS metric $C(d)$ and CFS metric $I(d)$ for a given d are:

$$C(d) = \max_k\{\mathbf{Z}_d(k)\} \tag{13}$$

$$I(d) = \arg\max_k\{\mathbf{Z}_d(k)\}, \quad k = [0 \sim 2047] \tag{14}$$

Then CTS and CFS is achieved as:

$$d_{est} = \arg\max_d\{C(d)\} \tag{15}$$

$$\nu_{I,est} = \begin{cases} I(d_{est})/2 & 0 \leq I(d_{est}) < 1024 \\ [I(d_{est}) - 2048]/2 & 1024 \leq I(d_{est}) < 2048 \end{cases} \tag{16}$$

which means the normalized estimation range of our CFS is ± 512. For P1 detection, an experimentally found threshold on $C(d)$ is reliably used, which we will not further discuss due to limited space.

Since the receiver does not know which P1 symbol is transmitted, we replace $\mathbf{x}_p$ by $\mathbf{x}_{128}$ to process the described correlation in practical use. Taking advantage of the correlation properties of $\mathbf{x}_{128}$ mentioned in Section 2, $C(d)$ will be a high value iff there is a P1 symbol in the received signal and $d = 0$, but is small otherwise.

To summarize, the main advantages of the proposed CTS and CFS are:

- down-shifting $C2$ and $B2$ zones by f_{sh} is avoided, thus the proposed method is insensitive to f_{sh} offset;
- the proposed method is insensitive to CW interference since the power of f_{cw} will spread to all the frequencies in $\mathbf{x}_p^*$ after correlating, thus it hardly exceeds the power of ν in $\mathbf{z}_0$, while in [4] a interference deleting process is required.
- numerical results show that the proposed CTS is good at locking to the correct timing in AWGN channel and the first main path in multipath Rayleigh fading channel.

3.2. Fine frequency synchronization (FFS)

After performing CTS and CFS, we obtain coarse CFO $\nu_{i,est}$ compensated $\mathbf{y}_0$ and $\mathbf{z}_0$ with residual $\nu_f \leq \pm 0.25$. Without noise:

$$\mathbf{z}_0(i) = |\mathbf{x}_p(i)|^2 \exp(j2\pi \frac{i\nu_f}{1024}), \quad i = [0 \sim 2047] \tag{17}$$

FFS is processed through a two-branch method similar to [4]:

$$P_c = \sum_{i=0}^{541} \mathbf{z}_0^*(i)\mathbf{z}_0(i+542) = e^{j2\pi\frac{542\nu_f}{1024}} \sum_{i=0}^{541} |\mathbf{p}(i)|^4$$

$$P_b = \sum_{i=1084}^{1565} \mathbf{z}_0^*(i)\mathbf{z}_0(i+482) = e^{j2\pi\frac{482\nu_f}{1024}} \sum_{i=542}^{1023} |\mathbf{p}(i)|^4$$

$$\nu_{f,est} = \arg(P_c \cdot P_b) \,/\, 2\pi \tag{18}$$

One can also estimate ν_f using $\mathbf{y}_0$ as described in [4], but the f_{sh} offset will need to be considered again. The FFS performance degradation by using $\mathbf{z}_0$ and $\mathbf{x}_{128}$ is less than 0.1dB.

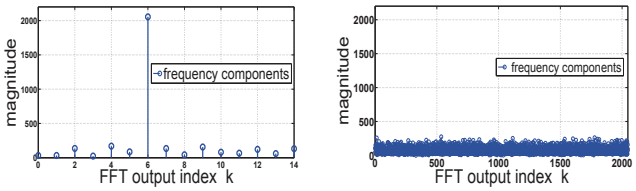

(a) correct timing (b) wrong timing

Fig. 2. FFT output under different timings, $\nu = 3$, SNR=-6dB

3.3. Time domain decoding

Time domain decoding is achieved by calculating the correlation between CFO compensated $\mathbf{y}_0$ with each of the 128 P1 symbols $\mathbf{x}_{0\sim127}$ and then finding out which $\mathbf{x}_k$ achieves the maximum:

$$R(k) = \sum_{i=0}^{2047} \mathbf{y}_0(i)\mathbf{x}_k^*(i), \quad k = [0 \sim 127] \tag{19}$$

$$k_{est} = \arg\max_k R(k) \tag{20}$$

Two methods are available to reduce computation load:

- correlate $i \in [C1 \sim B1]$ zone only, the correlation property in $[C1 \sim B1]$ is the same as in $[C2 \sim B2]$;
- split $\mathbf{x}_{0\sim127}$ into subgroups and correlating $\mathbf{y}_0$ with the average of each subgroup to identify which subgroup $\mathbf{y}_0$ is in. It requires at most $\log_2 128 = 7$ comparisons and can be further reduced to 5 comparisons since only 24 patterns are currently in use. On the other hand, such averaging is not applicable to binary sequences in post-FFT decoding.

3.4. Refining FFS, CIR estimation and fine timing synchronization (FTS)

After decoding, we can do FFS again using $\mathbf{y}_0$ and the exact $\mathbf{x}_p$ instead of $\mathbf{x}_{128}$. This process is optional since the former one is precious enough.

CIR estimation using $\mathbf{y}_0$ and $\mathbf{x}_p$ for FTS is needed in multipath fading channel as the last step of synchronization. Due to limited space, we do not discuss it here. Interested readers may refer to [2].

4. NUMERICAL RESULTS

The proposed method is computer simulated under an 8MHz baseband OFDM system with 2K normal OFDM symbols over AWGN and multipath Rayleigh fading channels given in [4]. For fading channel we make sure that channel taps are T-spaced (Tab. 1). We evaluate CTS, CFS, FFS and decoding performance using all the 128 and currently used 24 P1 symbols (thus the coarse P1 symbol is the average of $\mathbf{x}_{0\sim23}$ in this case), respectively. CFO ν is assumed to be 3.3. To obtain reliable results, at least 50 decoding errors are processed for each SNR point.

Fig. 3 gives CTS performance of the proposed method. We first show the mean square error (MSE) of d_{est}. The MSE of the proposed CTS method decreases rapidly with increasing SNR. We further demonstrate the probability that d_{est} is not 0 for AWGN channel and in the range $[0 \sim 15]$ for fading channel, respectively. The proposed CTS is good at locking to the correct timing in AWGN channel. After SNR of 10dB, the locking failure rate is less then 0.1%. For fading channel, we observe that the proposed method is good at

tap	0	1	3	4	5	7
ρ	0.248	0.129	0.31	0.425	0.49	0.0365
ϕ	-2.57	-2.12	0.35	0.42	2.72	-1.44
tap	8	12	17	24	29	49
ρ	0.12	0.2	0.419	0.317	0.2	0.185
ϕ	1.13	-0.81	-1.55	-2.22	2.84	2.86

Table 1. Multipath Rayleigh fading channel parameters

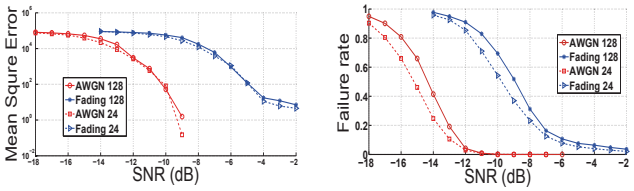

(a) MSE of CTS (b) Failure rate of CTS

Fig. 3. CTS performance

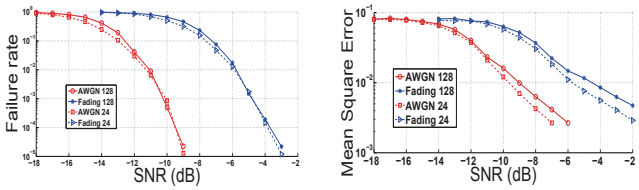

(a) Failure rate of CFS (b) MSE of FFS

Fig. 4. CFO performance

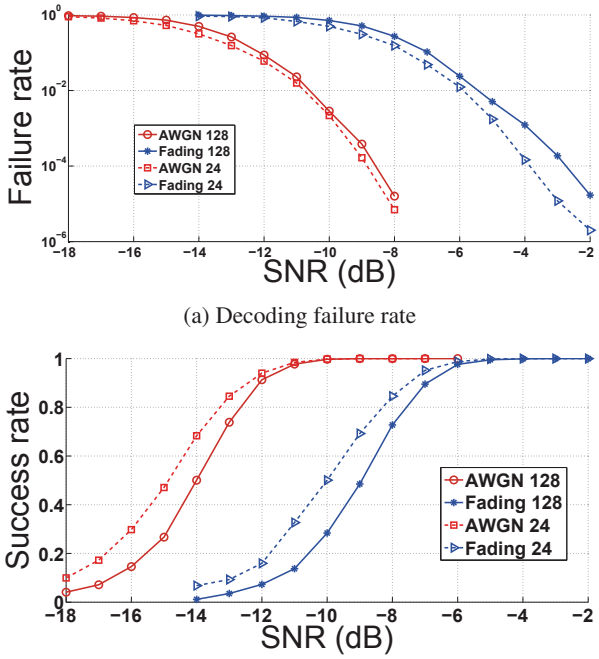

(a) Decoding failure rate

(b) Decoding success rate

Fig. 5. Decoding performance

locking to the first main path which has a large channel gain. However, since the first main path is not necessarily in the range $[0 \sim 15]$, we observe an error floor of locking failure rate in fading channel. The same reason explains the MSE floor in Fig. 3(a).

Fig. 4 shows frequency synchronization performance. Since $\nu = 3.3$, both 3 and 3.5 are acceptable values for CFS. Hence we plot in Fig. 4(a) the probability that the estimated v_I is neither 3 nor 3.5. The CFS failure rate with an SNR higher than -10dB in AWGN channel and -4.8dB in fading channel is less than 0.1%. The MSE of FFS is given in Fig. 4(b), which decreases exponentially with SNR.

Fig. 5 shows the decoding performance. We announce "success" when both $S1$ and $S2$ are correctly decoded. In Fig. 106 and 107 of [4], the decoding success rate of $S1$ and $S2$ approaches 1 at an SNR of -4dB in both AWGN and fading channels; but in the proposed method, this value is -10dB in AWGN and -6dB in fading channels, i.e., an SNR gain of 6dB and 2dB is achieved, respectively. If we use 24 patterns only, a slightly better performance can be obtained.

5. CONCLUSION

This paper presented a new time domain synchronization and decoding method for the P1 symbol in DVB-T2 based on the correlation between the received signal and time domain P1 symbols without post-FFT decoding. The proposed method achieves good synchronization performance and also decoding SNR gain compared to the scheme given in the standard guidelines. This paper suggested a frequency search method which is not based on trial-and-error. The suggested time domain decoding technique can be an alternative to the standard post-FFT one. Moreover, when we use FPTC techniques on normal OFDM symbols with non-unique pilot patterns, our "coarse symbol" method enables to reduce the system complexity by shortening the working sequence in [3] to 1 OFDM symbol and by avoiding pilot pattern selection in [2].

6. REFERENCES

[1] X. Wang, Y. Wu, and J. Chouinard, "A channel characterization technique using frequency domian pilot time domain correlation method for DVB-T systems," *IEEE Transactions on Consumer Electronics*, vol. 49, no. 4, pp. 949–957, 2003.

[2] A. Filippi and S. Serbetli, "OFDM symbol synchronization using frequency domain pilots in time domain," *IEEE Transactions on wireless communications*, vol. 8, no. 6, pp. 3240–3248, June 2009.

[3] B. Jahan, M. Lanoiselee, G. Degolet, and R. Rabineau, "Frame synchronization method for OFDM/OWAM and OFDM/QAM modulation," *IEEE International Conference on Circuit and Systems for Communications 2008, Shanghai,China*, May 2008.

[4] DVB Document A133, "Implementation guidelines for a second generation digital terrestrial television broadcasting system (DVB-T2)," 2010.

[5] DVB Document A122, "Frame structure, channel coding and modulation for a second generation digital terrestrial television broadcasting system (DVB-T2)," 2008.

[6] F. Classen and H. Meyr, "Frequency synchronization algorithms for OFDM systems suitable for communication over frequency selevtive fading channels," *IEEE 44th Vehicular Technology Conference*, vol. 3, pp. 1655–1659, 1994.